

Photoreactions of Phenylborylene with Dinitrogen and Carbon Monoxide

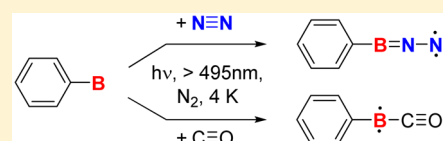
Klara Edel,[†] Matthias Krieg,[†] Dirk Grote,[‡] and Holger F. Bettinger^{*,†}

[†]Institut für Organische Chemie, Universität Tübingen, Auf der Morgenstelle 18, 72076 Tübingen, Germany

[‡]Lehrstuhl für Organische Chemie II, Ruhr-Universität Bochum, Universitätsstr. 150, 44780 Bochum, Germany

S Supporting Information

ABSTRACT: Formal removal of two bonding partners from boranes, BR_3 , yields borylenes, RB , which have been inferred as reactive intermediates in a number of reactions. Phenylborylene ($R = C_6H_5$; **1**) is accessible from phenyldiazidoborane by photochemical extrusion of dinitrogen under matrix isolation conditions. Concomitantly, the nitrene $PhNBN$ is formed via phenyl rearrangement. Here we used a combination of UV/vis, IR, and ESR spectroscopy under cryogenic matrix isolation conditions to investigate the properties and reactivity of phenylborylene. We detected an absorption band of phenylborylene at 375 nm ($S_0 \rightarrow S_2$) and tentatively assigned the $S_0 \rightarrow S_1$ transition to a very weak band at 518 nm. We also show for the first time that an electrophilic borylene such as **1** can react with N_2 reversibly and with CO irreversibly under photochemical conditions. The corresponding photoproducts $PhBNN$ and $PhBCO$ have triplet electronic ground states. Their small E values are in agreement with the linear arrangements $Ph-B-N-N$ and $Ph-B-C-O$ obtained by density functional theory computations. The D values decrease in the series $PhNBN > PhBNN > PhBCO$ and approach the value for phenylcarbene ($PhCH$). Indeed, the boron center in $PhBCO$ is isoelectronic with the carbene center in $PhCH$. The compounds are the first examples of boron analogues of diazoalkanes (R_2CNN) and ketenes (R_2CCO), and their formation may serve as a demonstration of the high reactivity of phenylborylene.



INTRODUCTION

The boron analogues of carbenes, borylenes, which are also known as borenes or boranediyls, are an underrepresented class of reactive intermediates in the chemical literature. This is not due to a lack of interest in these fundamental species of boron chemistry but rather to the difficulties in obtaining them. For example, early claims¹ of methylborylene (CH_3B) generation by reductive elimination of dibromomethylborane (CH_3BBr_2) were later on refuted.^{2,3} Likewise, the reported photochemical generation of (1-naphthyl)borylene from tris(1-naphthyl)borane⁴ was shown to be incorrect.⁵

A number of trapping experiments were interpreted as evidence for the involvement of borylenes. Timms, for example, obtained 1,4-diboracyclohexadiene derivatives from trapping of BF and BCl with ethyne (Scheme 1a).^{6–9} The borylenes were obtained by comproportionation of the corresponding trihalides over solid boron at very high temperatures. Pachaly and West¹⁰ ascribed the products obtained from photolysis of trisilylboranes in organic glasses in the presence of bis-(trimethylsilyl)acetylene at 77 K to result from trapping of silylborylenes (Scheme 1b). Curiously, the authors could not obtain spectral evidence for the formation of silylborylenes in the organic glass by optical spectroscopy.¹⁰ Grigsby and Power¹¹ reduced sterically encumbered arylboron dihalides and interpreted the isolated products as resulting from insertion of a transient borylene into a $C-C$ σ bond (Scheme 1c). Tokitoh and co-workers¹² photolyzed sterically encumbered bis(methylseleno)arylboranes in the presence of 1,2-diketones. The isolated 1,3,2-dioxaboroles were ascribed to result from the

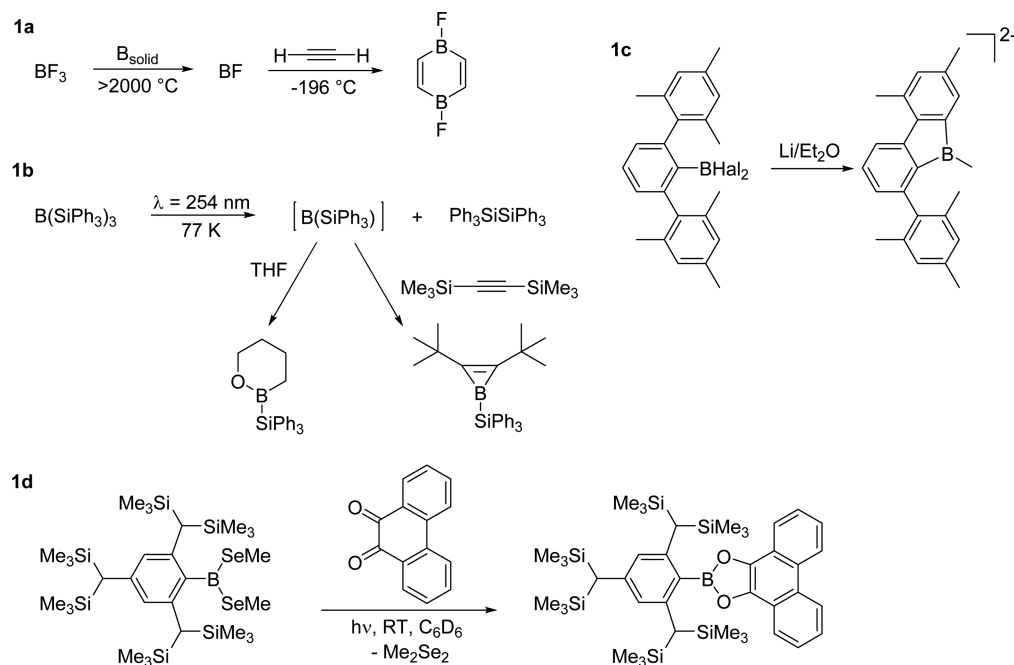
reaction of the transient arylborylene with the 1,2-diketone (Scheme 1d).¹²

The reductive elimination of the adducts of dichloroboranes and N-heterocyclic carbenes (NHCs) was investigated more recently.^{13,14} The reduction of a $mes_2BB(Cl)_2NHC$ with potassium graphite yielded the product that was ascribed to result from intramolecular CH insertion of a $R_2BB-NHC$ species (Scheme 2a).¹³ The reduction of $NHC-BHCl_2$ with sodium naphthalide produced a cycloadduct that was inferred to result from cycloaddition of $NHC-BH$ to naphthalene (Scheme 2b).¹⁴ This interpretation was challenged, however, and a boryl radical mechanism was suggested instead.¹⁵ An interesting recent observation is the CO extrusion from $ArB(CO)(CAAC)$ ($CAAC =$ cyclic (alkyl)(amino)carbene) to give the $ArB(CAAC)$ adduct, which was trapped intramolecularly or by an added neutral donor L (Scheme 2c).¹⁶

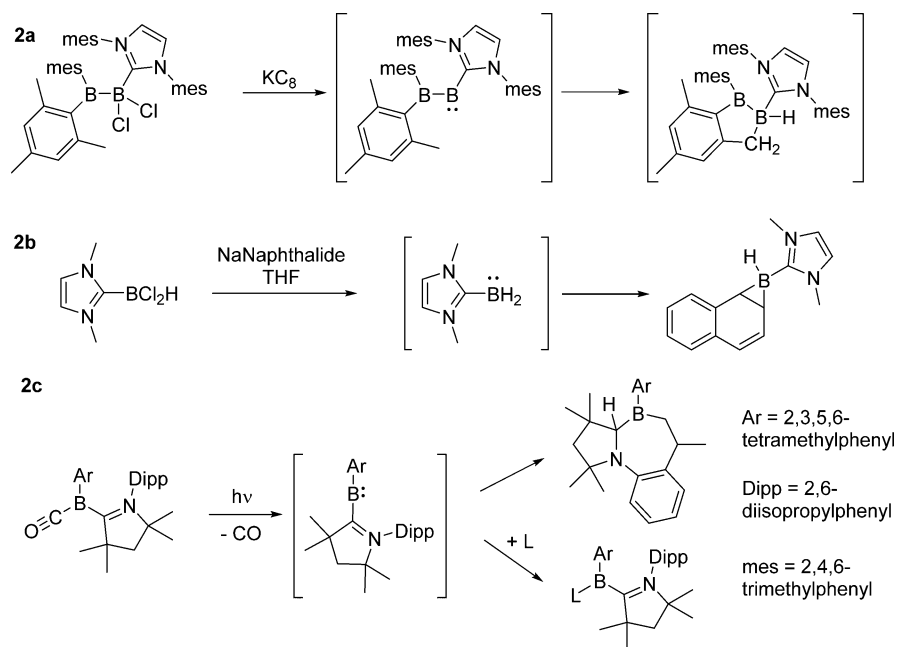
The reactant in Scheme 2c is an example of compounds of the type RBL_2 , with L being a neutral formal two-electron donor, which are currently receiving some attention as summarized in a recent review.¹⁷ When, e.g., a $CAAC$ or CO is used as a neutral donor, stable compounds RBL_2 ^{18,19} or RBL ^{20,21} result. These were considered as having boron in the formal oxidation state +1 and hence were perceived as stabilized borylenes. The boron center has lost its electrophilic nature and acts as a Brønsted or Lewis base toward a proton or a Lewis acid.^{18,22}

Received: August 10, 2017

Scheme 1. Trapping Experiments of Borylenes



Scheme 2. Trapping Experiments of Borylene–NHC or Borylene–CAAC Adducts



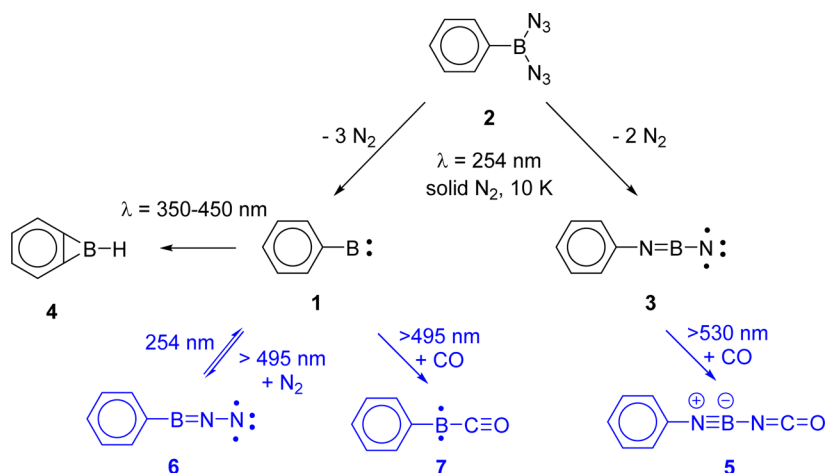
Direct spectroscopic observation of organoborylenes, RB, is extremely scarce. Andrews et al.²³ observed by IR spectroscopy that cocondensation of laser-ablated boron atoms and acetylene in an argon matrix gives ethynylborylene next to a number of additional products. We have reported that phenylborylene (**1**) can be obtained by UV photolysis of phenyldiazidoborane (**2**) in a nitrogen matrix along with nitrene **3** (Scheme 3).²⁴ The subvalent organoboron compound **1** was found to be photolabile, as longer-wavelength irradiation resulted in the formation of benzoborirene (**4**).²⁴ A computational analysis of various PhBN_x isomers identified **3** as the thermodynamically least stable isomer of PhBN₂ stoichiometry and the trans-

formation **2** → **1** + 3 N₂ as considerably exothermic (−21 kcal mol^{−1}).²⁵

The available experimental evidence from trapping studies suggests that borylenes RB are highly reactive transient species. Computational analysis of the reactions with prototypical carbon multiple bonds has revealed that borylenes behave as electrophilic species because of their vacant p orbitals.^{26,27} The transition states for cycloaddition resemble those of carbenes, and changes in barrier heights, distances, and angles can similarly be associated with varying borylene philicities.^{26,27}

In our preliminary report,²⁴ we focused on IR characterization of the products formed from **2** upon irradiation. We now report and discuss the observations from UV/vis and

Scheme 3. Photochemical Decomposition of Phenyl diazidoborane (2) Isolated in Solid Nitrogen at 10 K Results in Phenylborylene (1), *B*-Nitreno-*N*-phenyliminoborane (3), and Benzoborirane (4); The Reactions and Reaction Products *B*-Isocyanato-*N*-phenyliminoborane (5), *N*-Nitreno-*B*-phenyliminoborane or Phenyl diazoborane (6), and Phenylboraketene (7) (Drawn in Blue) Are the Subject of the Present Work



electron spin resonance (ESR) spectroscopy along with additional IR measurements in a nitrogen matrix as well as in a CO-doped nitrogen matrix. The experimental investigations are further complemented by detailed computational investigations. We report for the first time spectroscopic evidence for the photoreaction of phenylborylene with the N₂ and CO molecules (Scheme 3, blue part). The products PhBL (L = N₂, CO) are shown to have triplet ground states.

RESULTS AND DISCUSSION

UV/Vis Spectroscopy. Diazide 2 has its absorption of maximum intensity at 250 nm in solid nitrogen (Figure S1). Irrespective of the conformation of diazide 2, a strong absorption ($S_0 \rightarrow S_2$) is computed in the 4.5–4.6 eV (270–280 nm) range (Table S5). A much weaker (by a factor of 100) absorption ($S_0 \rightarrow S_1$) is obtained at longer wavelengths (272–292 nm). It is thus assumed that the strong band is due to the $S_0 \rightarrow S_2$ transition.

Irradiation was performed with the output of a low-pressure mercury lamp ($\lambda = 254$ nm). Under these conditions, a decrease of the diazide band (250 nm) was accompanied by a growth of signals due to 3 (709, 623, 557, 504, 413, 325, and 317 nm) and 1 (375 nm) (Figure 1). The assignments are based on the behavior of the bands in subsequent irradiations at various wavelengths in the absence and presence of small amounts of CO (up to 5%), complementary IR and ESR spectroscopy, and computations as detailed below.

The bands assigned to 3 decreased upon irradiation into the long-wavelength transitions ($\lambda > 530$ nm) in the presence of CO (Figure 2). Although no characteristic new bands were observed in the UV/vis spectra, the formation of the isocyanate PhNB(NCO) (5) was confirmed by IR spectroscopy (see below). The only band growing under these irradiation conditions is at around 250 nm. The isocyanate has its strongest and longest-wavelength absorption at 265 nm ($f = 0.472$), and hence, experiment and theory are in agreement with respect to the changes in the optical spectra under these irradiation conditions ($\lambda > 530$ nm) in the presence of CO. In the absence of CO, only slight bleaching of the bands associated with 3 was observed upon $\lambda > 530$ nm irradiation (Figure 1). There is some similarity to the photochemical

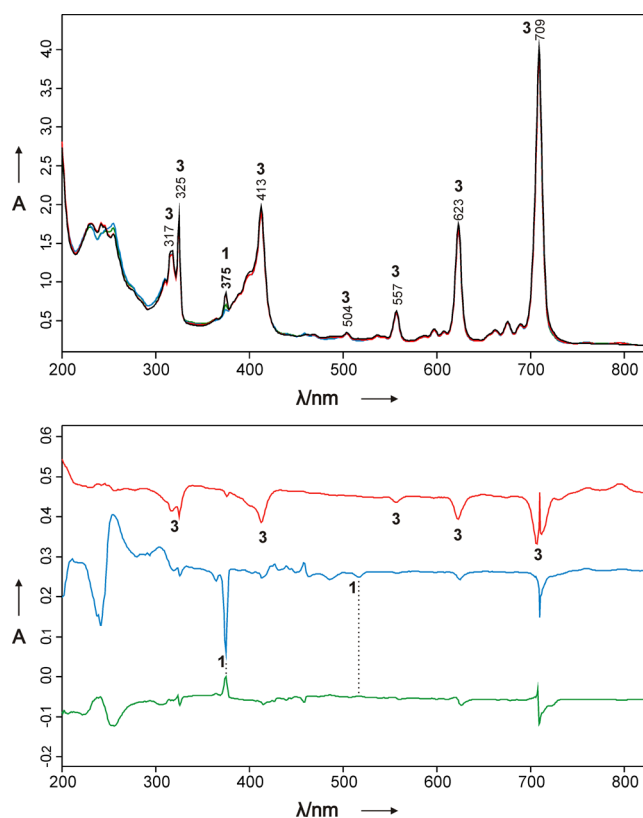


Figure 1. UV/vis spectra of the photodecomposition of diazide 2. The UV/vis spectrum of diazide 2 is not shown. Top panel: black trace, after irradiation of a nitrogen matrix containing diazide 2 for 35 min at $\lambda = 254$ nm; red trace, after irradiation of the black trace for 2 h at 530 nm $< \lambda < 630$ nm; blue trace, after irradiation of the red trace at 495 nm $< \lambda < 630$ nm for 1 h; green trace, after irradiation of the blue trace at $\lambda = 254$ nm for 25 min. Bottom panel: difference spectra (bands pointing downward decrease and bands pointing upward increase during irradiation): red trace, after irradiation at 530 nm $< \lambda < 630$ nm for 2 h; blue trace, after irradiation at 495 nm $< \lambda < 630$ nm for 1 h; green trace, after irradiation at $\lambda = 254$ nm for 25 min.

behavior of the triplet borylnitrene CatBN (Cat = catecholato), which upon long-wavelength irradiation was found to react

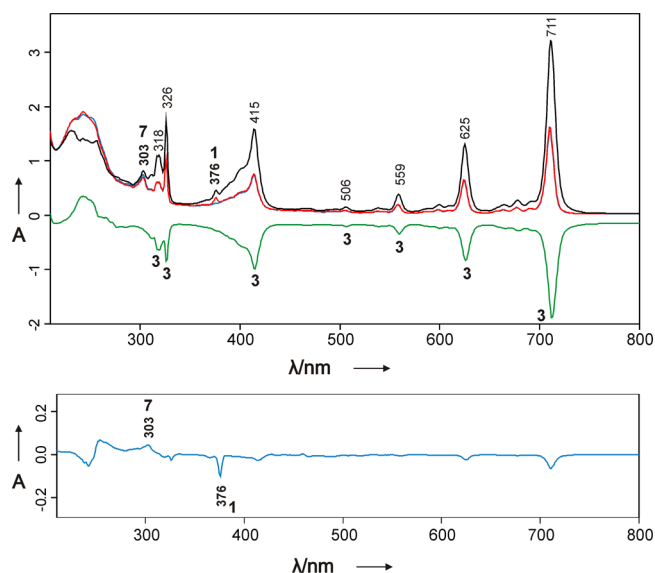


Figure 2. UV/vis spectra of the photodecomposition of diazide **2** in a CO (5%) doped N_2 matrix. UV/vis spectrum of diazide **2** is not shown. Top panel: black trace, after irradiation of diazide **2** for 33 min at $\lambda = 254$ nm; red trace, after irradiation of the black trace for 2 h at 530 nm $< \lambda < 630$ nm; blue trace, after irradiation of the red trace at 495 nm $< \lambda < 630$ nm for 1 h; green trace, difference spectrum obtained from the red and black traces showing decreasing signals of **3**. Bottom panel: difference spectrum obtained from the blue and red traces in the top panel, showing the decreasing signal of **1** and increasing signal of **7**. In the difference spectra, bands pointing downward decrease and bands pointing upward increase during irradiation.

readily with N_2 to form its azide $CatBN_3$ and with CO to form its isocyanate $CatB(NCO)$.²⁸

The absorption spectrum of **3** computed at the TD-B3LYP level places the $S_0 \rightarrow S_2$ transition at 2.0 eV (634 nm) with considerable oscillator strength. The experimental transition energy (1.7 eV, 709 nm) is in reasonable agreement with the computations. The $S_0 \rightarrow S_1$ transition of **3** (1.6 eV) is not dipole-allowed because S_1 is 1^3A_1 according to these computations. The spacings between the signals in the visible are 1947, 1902, and 1888 cm^{-1} , indicating that the three bands of lower intensity (623, 557, and 504 nm) are due to a vibronic progression that is associated with the BN stretching vibration of **3**. Low-energy excited states (up to 600 nm) and a pronounced vibrational progression were also observed in the absorption spectrum of the triplet borylnitrene $CatBN$ in argon.²⁸

The band at 375 nm was the only signal that did not change intensity upon $\lambda > 530$ nm irradiation in the presence of CO (Figure 2). However, the signal was quickly bleached in the absence of CO upon shorter-wavelength irradiation ($\lambda = 350$ – 450 nm), while the other bands associated with **3** were hardly affected. We have previously shown by IR spectroscopy that 350–450 nm irradiation results in the photoreaction of **1** to form **4**.²⁴ Hence, the feature at 375 nm is assigned to **1**. A computational investigation of the low-lying excited states of various borylenes was reported recently.²⁹ For borylenes such as **1**, two low-energy excited states, 1^1B_1 (S_1) and 1^1B_2 (S_2), exist as a result of excitation from the HOMO ($13a_1$) to the LUMO ($3b_1$) or LUMO+1 ($8b_2$). The stronger absorption is due to the $S_0 \rightarrow S_2$ transition that is computed for **1** at 392 nm (TD-B3LYP, $f = 0.041$).²⁹ The $S_0 \rightarrow S_1$ transition is weaker by

a factor of 4 and is expected to appear at much longer wavelengths (529 nm).²⁹ The long-wavelength absorption of **1** was difficult to detect in our experiments, and it is tentatively assigned to a very weak band at 518 nm that shows the same behavior as the band at 375 nm in irradiation experiments. The presence of the weak band of **1** can be demonstrated by irradiation with light of wavelength $\lambda > 495$ nm after first irradiating with $\lambda > 530$ nm. Under these irradiation conditions, the 375 nm band decreases quickly while the bands of **3** are hardly affected (Figure 1). This photoreaction is partially reversible, and irradiation with 254 nm light resulted in growth of the signals of **1** (Figure 1). Complementary IR and ESR experiments (see below) demonstrated that these conditions resulted in the photoreaction of **1** with N_2 to give $PhB(NN)$ (**6**). Bands grew in the 250–260 nm region, around 305 nm, and at 459 nm (2.7 eV). Computations for **6** arrived at a weak band at 3.1 eV (396 nm, $f = 0.047$) and a stronger one at 4.0 eV (311 nm, $f = 0.120$), in reasonable agreement with the experimental observations.

Shorter-wavelength irradiation ($\lambda > 495$ nm) in the presence of CO, i.e., into the very weak transition of **1**, also resulted in the disappearance of the bands of **1** (Figure 2). Under these conditions, a single band at 303 nm grew. IR and ESR spectroscopy (discussed below) demonstrated that the product of the photoreaction of **1** with CO is $PhB(CO)$ (**7**). Computations were in agreement with assignment of the 303 nm band to **7**, as the strongest absorption was computed to be at 306 nm ($f = 0.320$). Further discussion of the electronic structures of **6** and **7** is presented below.

IR Spectroscopy. The previous IR spectroscopic investigation found that irradiation at $\lambda = 350$ – 450 nm turned **1** into **4**.²⁴ In the 1417–1387 cm^{-1} range a number of weak bands that could not be assigned at that time also increased under these irradiation conditions.²⁴ As we deduced from the UV/vis experiments and the computations²⁹ that there are two low-lying excited states of **1** (see above), we irradiated the mixture of **1** and **3** with long-wavelength light. Upon >530 nm irradiation, **1** was photostable while IR bands associated with **3** were hardly changed (Figure 3). Upon >495 nm irradiation, the bands of **1** quickly decreased in intensity and new signals grew. These bands do not belong to **4** but are assigned to **6** on the basis of computations and isotopic labeling studies using $^{15}N_2$. The IR signals for ^{15}N -labeled **6** are observed at 1373–1367 cm^{-1} . The measured isotopic shift of approximately 25–28 cm^{-1} is in agreement with the computed one (24.9 cm^{-1}). The band of the $\nu(BNN)$ stretching vibration is tentatively assigned to the feature observed at 1691 cm^{-1} (1752.8 cm^{-1} calculated at the B3LYP/6-311+G** level). However, the band for the isotopically labeled compound $PhB(^{15}N^{15}N)$ could not be assigned because of overlap with other signals. As observed by UV/vis spectroscopy, the photoreaction $PhB + N_2$ is reversible upon 254 nm irradiation, as the signals due to **6** decreased while those of **1** increased in intensity (Figure 3).

In a CO-doped N_2 matrix, nitrene **3** reacts with CO upon >530 nm irradiation to form $PhB(NCO)$, as shown by the growth of the typical isocyanate bands at 2315–2332 cm^{-1} and the stretching vibration of the iminoborane unit (Figure 4). The latter band shows the typical 1:4 intensity ratio of the ^{10}B and ^{11}B isotopologues at 2131 and 2081 cm^{-1} . The assignment is supported by the finding that the isocyanate band shifts upon isotopic substitution (60–61 cm^{-1} for ^{13}CO and 16–17 cm^{-1} for $C^{18}O$) while the iminoborane stretching vibration is essentially insensitive. The observed isotopic shifts are in

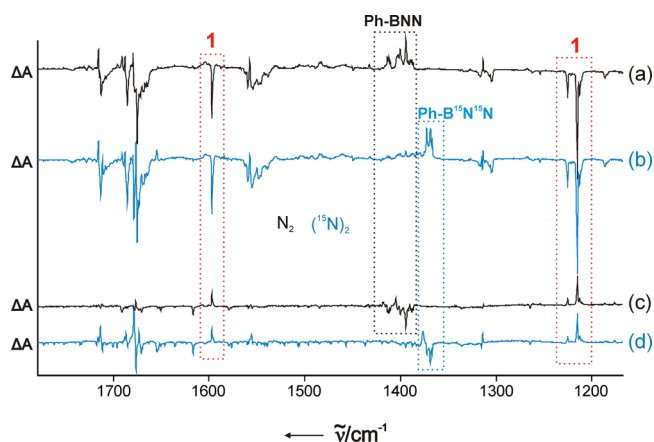


Figure 3. IR difference spectra showing the photoreversible reaction between **1** and **6**. Signals of **1** are framed in a red box. Black traces show spectra of a dinitrogen matrix and blue traces those of a $^{15}\text{N}_2$ matrix. Before irradiation at $495\text{ nm} < \lambda < 630\text{ nm}$, matrices containing diazide **2** were irradiated at $\lambda = 254$ and $530\text{--}630\text{ nm}$. (a, b) Difference spectra after irradiation at $495\text{ nm} < \lambda < 630\text{ nm}$ for 80 min; (c, d) difference spectra after irradiation at $\lambda = 254\text{ nm}$ for 30 min. In the difference spectra, bands pointing downward decrease and bands pointing upward increase during irradiation.

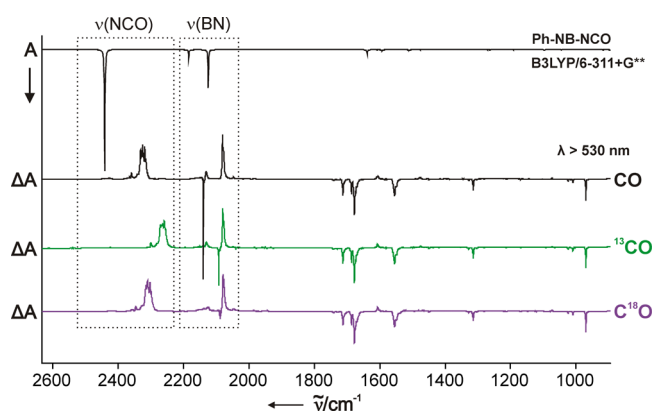


Figure 4. IR difference spectra showing the photoreaction between **3** and CO to form **5** through irradiation at $530\text{ nm} < \lambda < 630\text{ nm}$ for 2 h in a dinitrogen matrix doped with 5% isotopically labeled carbon monoxide. Before irradiation at $530\text{ nm} < \lambda < 630\text{ nm}$, matrices containing diazide **2** were irradiated at $\lambda = 254\text{ nm}$ for 30 min. The top trace shows a spectrum of **5** computed at the B3LYP/6-311+G** level of theory. In the difference spectra, bands pointing downward decrease and bands pointing upward increase during irradiation.

agreement with those computed for **5** (63.4 cm^{-1} for ^{13}CO and 13.6 cm^{-1} for C^{18}O , see Table S1). Interestingly, computations arrived at a linear structure for this isocyanate (see Figure S2). This is most likely due to the adjacent electron-deficient dicoordinate boron center, similar to the situation in electron-deficient linear ketenimines.³⁰ While isocyanates of iminoboranes were not considered previously, dimethylisocyanatoborane, $(\text{CH}_3)_2\text{BNCO}$, was found to feature a bent isocyanato group with a very low barrier for isomerization,³¹ in agreement with our computations (see Figure S2).

After much of nitrene **3** was converted to **5**, switching the wavelength of irradiation to $>495\text{ nm}$ resulted in a quick decrease of the bands of **1** and the growth of a set of new signals (Figure 5). The photoproduct is assigned to boraketene **7** on the basis of isotopic shifts (^{13}CO and C^{18}O) and comparison with computed harmonic vibrational frequencies.

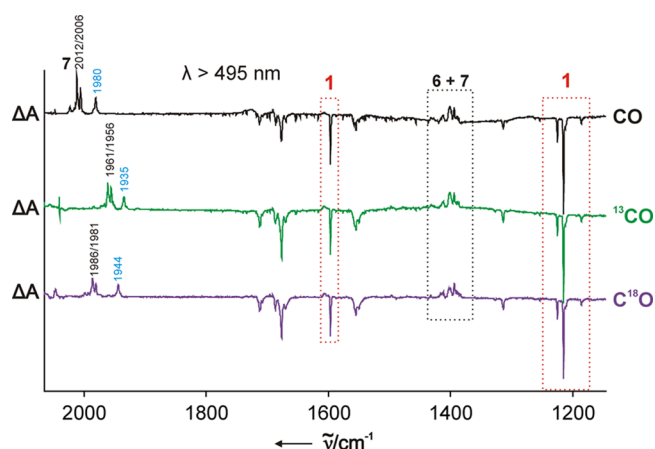


Figure 5. IR difference spectra showing the photoreaction between **1** and CO to form **7** through irradiation at $495\text{ nm} < \lambda < 630\text{ nm}$ for 1 h in a dinitrogen matrix doped with 5% isotopically labeled carbon monoxide. Before irradiation at $495\text{ nm} < \lambda < 630\text{ nm}$, matrices containing diazide **2** were irradiated at $\lambda = 254\text{ nm}$ for 30 min and at $530\text{--}630\text{ nm}$ for 2 h. Decreasing signals of **1** are framed in a red box. In the difference spectra, bands pointing downward decrease and bands pointing upward increase during irradiation.

The same set of signals was already observed in the previous irradiation of the same CO-doped matrix at $\lambda = 254\text{ nm}$. The signals at $2012/2006\text{ cm}^{-1}$ belong to the $\nu(\text{BCO})$ stretching vibration and show isotopic shifts of 51 and 26 cm^{-1} upon the use of ^{13}CO and C^{18}O , respectively, in good agreement with the computed values of 52.8 and 26.1 cm^{-1} for $\text{PhB}(^{13}\text{CO})$ and $\text{PhB}(\text{C}^{18}\text{O})$, respectively, obtained at the B3LYP/6-311+G** level of theory. Signals around 1400 cm^{-1} overlap with signals of **6** which is formed under the same irradiation conditions because of the presence of an excess of dinitrogen in the matrix. Besides the signals of **7**, a new band at 1980 cm^{-1} was observed upon irradiation at $>495\text{ nm}$. This signal behaves differently than the signals of **7** upon irradiation at $\lambda = 254\text{ nm}$. Because of the shift of the band in the presence of ^{13}CO , its assignment to PhBO ($\tilde{\nu} = 1977\text{--}1971\text{ cm}^{-1}$ in Ar)³² is excluded. While the newly formed species cannot be assigned, we note that a possible candidate could be the bis-CO derivative $\text{PhB}(\text{CO})_2$ (Table S4).¹⁹

In summary, the behaviors of the bands assigned to **1** and **3** under various irradiation conditions are identical under both IR and UV/vis spectroscopic detection in support of the assignments to **1** and **3**.

ESR Spectroscopy. The earlier assignment of triplet **3** as the major product of photodecomposition of diazide **2** was based on IR spectroscopy and supported by an ESR spectroscopy investigation.²⁴ A triplet signal observed in argon with zero-field splitting (zfs) parameters $|D/hc| = 1.240\text{ cm}^{-1}$ and $|E/hc| = 0.0021\text{ cm}^{-1}$ was observed after extended irradiation ($\lambda = 254\text{ nm}$) and assigned to **3**.²⁴ In the present work, additional measurements were performed in solid nitrogen at 4 K. This results in slightly changed zfs parameters for **3** ($|D/hc| = 1.247\text{ cm}^{-1}$ and $|E/hc| = 0.002\text{ cm}^{-1}$).

An additional but much weaker signal with smaller zfs parameters (in argon,²⁴ $|D/hc| = 0.870\text{ cm}^{-1}$ and $|E/hc| = 0.0007\text{ cm}^{-1}$; in nitrogen, $|D/hc| = 0.882\text{ cm}^{-1}$ and $|E/hc| < 0.001\text{ cm}^{-1}$) was also observed after irradiation of **2** at $\lambda = 254\text{ nm}$. The carrier of this signal could not be firmly assigned in our previous investigation.²⁴ Monitoring the subsequent longer-wavelength irradiation ($\lambda = 350\text{--}450\text{ nm}$) by ESR spectroscopy

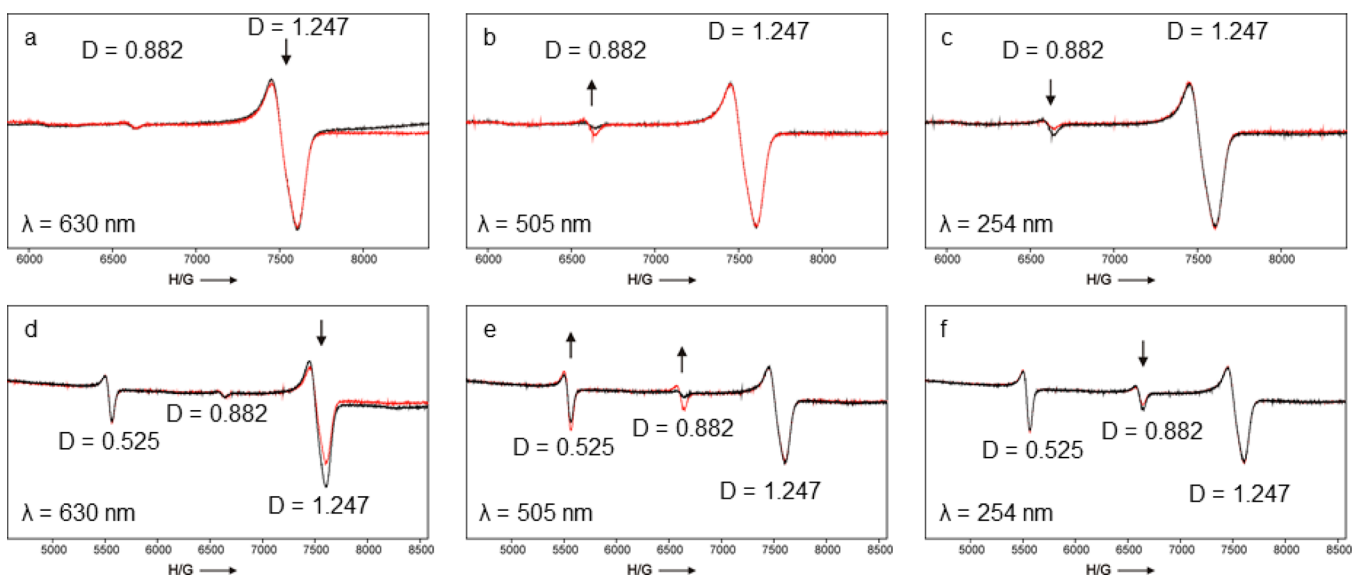


Figure 6. ESR spectra (4 K) obtained after 254 nm irradiation of **2** in (a–c) N_2 and (d–f) CO-doped N_2 (5%). Black, spectra before irradiation given in the panel; red, spectra after irradiation given in the panel. Arrows pointing up or down indicate an increase or decrease in the corresponding absorption under the irradiation conditions given.

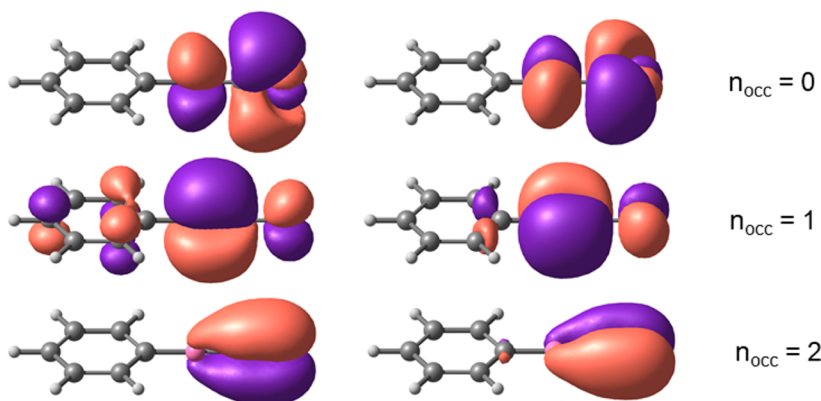


Figure 7. Natural orbitals and occupation numbers of the B–C–O unit of PhBCO (3A_2) computed at the UB3LYP/6-311+G** level of theory.

in the present work showed that the weak signal intensifies while the strong one associated with **3** stays almost constant (Figure S3). Under these irradiation conditions, **1** undergoes the photoreaction to form benzoborirene,²⁴ an ESR-silent singlet species, and reacts with N_2 to afford **6**, as shown above by IR spectroscopy. Switching the wavelength of irradiation to $\lambda = 308$ nm (XeCl excimer laser) reduces the intensity of the signal with the smaller D value, while the signal due to **3** again stays constant.

As the IR and UV/vis experiments showed wavelength-selective photochemistry of **3** (>530 nm) and **1** (>495 nm) in the absence or presence of CO, additional experiments were performed. In the absence of CO, irradiation at 630 nm using a light-emitting diode (LED) results in weakening of the ESR signal of **3** (Figure 6a), probably as a result of the reaction with N_2 to give PhNBN₃. Switching the irradiation wavelength to 505 nm (LED) causes an increase in the weaker signal (Figure 6b), while this signal decreases again upon short-wavelength irradiation (254 nm) (Figure 6c). As under long-wavelength irradiation conditions **1** reacts with molecular nitrogen to afford **6** and as this can be cleaved to **1** + N_2 upon short-wavelength irradiation according to IR and UV/vis measurements, the weak

ESR signal is assigned to the xy_2 transition of the triplet ground state of **6**, in agreement with the previous suggestion.²⁴

In the presence of CO, the strongest ESR signal is still due to **3** after photodecomposition of the diazide by 254 nm irradiation (Figure 6d). This strongest signal decreases in intensity upon irradiation with 630 nm light (Figure 6d). This observation is in agreement with the IR and UV/vis measurements and is due to the formation of isocyanate **5**. Besides the weak signal of **6**, another triplet signal ($|D/hc| = 0.525$ cm⁻¹ and $|E/hc| < 0.0005$ cm⁻¹) of higher intensity can be observed already after 254 nm irradiation (Figure 6d). The signal of medium intensity and that of **6** increase upon 505 nm irradiation (Figure 6e). Upon short-wavelength irradiation, only the signal of **6** decreases (Figure 6f). As the IR and UV/vis measurements confirmed the formation of **6** and **7** under these irradiation conditions, the new signal is assigned to the latter compound. The small E value (<0.0005 cm⁻¹) is indicative of a structure that is almost cylindrical, in agreement with the computed linear arrangement of the Ph–B–C–O unit.

The preference of a triplet electronic ground state (3A_2) for **3** and **6** was discussed previously on the basis of results obtained with multireference second-order perturbation theory (MRMP2).²⁵ Briefly, simple molecular orbital (MO) analysis

revealed that each of the two compounds features two orthogonal π systems with three π orbitals at the NBN or BNN termini that are almost degenerate. As each of the termini has six π electrons, a high-spin state results, and this was confirmed by the MRMP2 computations.²⁵ For isoelectronic 7 a similar electronic structure was expected and confirmed by computations (see the MOs in Figure 7).

The ground state of linear 7 is the 3A_2 state, while the 1A_2 and 1A_1 states are higher in energy by 10.1 and 12.0 kcal mol⁻¹ at the CASPT2-CAS(12,12)/cc-pVTZ//B3LYP/6-311+G** level of theory (Table 1). The triplet ground state of 7 is in line with the ESR spectroscopy experiments discussed above.

Table 1. Vertical Excitation Energies (in kcal mol⁻¹) Computed at the CASPT2-CAS(12,12)/cc-pVTZ//B3LYP/6-311+G Level of Theory**

compound	3A_2	1A_2	1A_1
PhNBN	0	16.1	18.5
PhBNN	0	15.5	18.2
PhBCO	0	10.1	12.0

The spin density at the terminal nitrogen center is larger in 3 than in 6 according to computations (Figure 8). This is in agreement with the larger $|D/hc|$ value of 3 (1.247 cm⁻¹), which is in the range that is typical for nitrenes with weak delocalization. For example, the closely related boryl nitrenes CatBN and PinBN (Pin = pinacolato) have $|D/hc|$ values of 1.49 and 1.57 cm⁻¹, respectively,^{28,33,34} while the $|D/hc|$ value for phenylnitrene is 0.99 cm⁻¹.³⁵ The spin density at the boron center is quite large in 6, and in agreement with the stronger delocalization, the $|D/hc|$ value is smaller (0.882 cm⁻¹). In comparison with 6, the spin density at the boron center is still larger in 7. The boron atom in 7 is isoelectronic to the carbon center in a carbene (RCR), and indeed, the $|D/hc|$ value of 0.525 cm⁻¹ is similar to that of phenylcarbene ($|D/hc| = 0.518$ cm⁻¹ in Fluorolube at 77 K).³⁶

CONCLUSIONS

The present investigation of the photodecomposition of phenyldiazidoborane (2) upon 254 nm irradiation showed

that phenylborylene (1) forms along with nitrene PhNBN (3), which is the major persistent photoproduct. PhNBN could be characterized by ESR, IR, and UV/vis spectroscopy. This nitrene absorbs in the visible region beyond 700 nm with rather sharp absorption bands and a pronounced vibrational progression. PhNBN reacts photochemically with CO upon >530 nm irradiation to give the linear isocyanate PhNB(NCO) (5).

Compound 1 is a minor product of the photodecomposition of 2. We could determine the energies of the two lowest-energy excited states, which are in the visible (tentatively 518 nm) and UV (375 nm) regions. This marks the first observation of the absorption energies of a borylene larger than a diatomic one and is expected to be very important for future transient absorption spectroscopy experiments with phenylborylene, in particular as the experimental observations confirm earlier computations.²⁹

Our study provides the first example of the direct observation of a reaction of a borylene (RB). Phenylborylene reacts under photochemical conditions with visible light (>495 nm) with N₂ and CO to give PhBNN (6) and PhBCO (7), respectively. The photoproducts are ground-state triplet species with a linear arrangement at the boron center according to ESR and computational investigations. The $|D/hc|$ value of 0.5 cm⁻¹ for 7 is similar to that of phenylcarbene (PhCH), showing that the isoelectronic relationship of the dicoordinate boron and carbon centers is also reflected in the electronic properties.

EXPERIMENTAL DETAILS

Synthesis and Handling of PhB(N₃)₂. CAUTION! Phenyl-diazidoborane is explosive. While no explosions were experienced in our laboratory, utmost care must be taken when handling the compound. We used a face shield, Kevlar gauntlets and gloves, and a leather apron. The compound was only prepared in small amounts (max. 10 mg) from commercially available dichlorophenylborane and chlorotrimethylsilane in dichloromethane following the procedure described by Mennekes and Paetzold.³⁷

Matrix Isolation Experiments. Matrix experiments were performed by standard techniques³⁸ using a SHI CKW-21A duplex closed-cycle helium cryostat (IR and ESR) and a CTI Cryogenics 8200 compressor (Brooks Automation) (UV). Phenyldiazidoborane was sublimed from a glass flask at 0 °C and condensed onto a cold CsI (IR) or sapphire (UV) window or on a copper rod (ESR) with a large

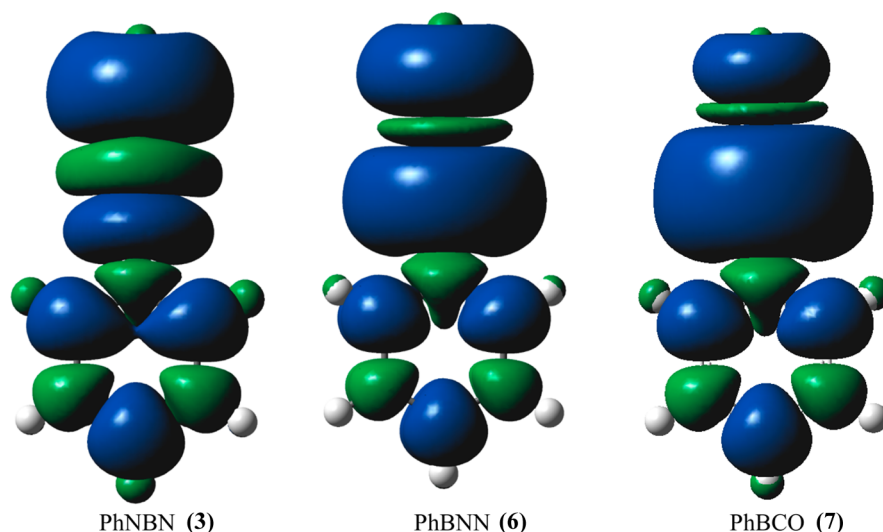


Figure 8. Computed (UB3LYP/6-311+G**) spin densities.

excess of dinitrogen 6.0 (Westfalen AG), $^{15}\text{N}_2$ 2.2 (Westfalen AG), or dinitrogen doped with 5% carbon monoxide 3.7 (Westfalen AG), C^{18}O 2.0 (95% ^{18}O) (Sigma-Aldrich), or ^{13}CO 2.3 (99.1% ^{13}C) (Westfalen AG). The gases or gas mixtures were dosed to 2.0 sccm (IR), 1.5 sccm (UV), or 3.5 sccm (ESR) by a mass flow controller (MKS mass flow PR400B). The deposition temperature was 28 K. FTIR spectra were measured between 4000 and 400 cm^{-1} on a Bruker Vertex 70 spectrometer using a resolution of 0.5 cm^{-1} . UV/vis spectra were measured on a PerkinElmer Lambda 1050 spectrophotometer. X-band ESR spectra were recorded on a Bruker Elexsys E500 ESR spectrometer with an ER077R magnet (75 mm pole cap distance), an ER047 XG-T microwave bridge, and an oxygen-free high-conductivity copper rod (75 mm length, 3 mm diameter) cooled by a closed-cycle cryostat. Computer simulations of the ESR spectra were performed using the XSophe computer simulation software suite (version 1.0.4),³⁹ developed by the Centre for Magnetic Resonance and Department of Mathematics, University of Queensland (Brisbane, Australia) and Bruker Analytik GmbH (Rheinstetten, Germany).

Irradiations were achieved with a low-pressure mercury lamp (VVP, 253.7 nm) and an Osram HBO-500-W/2 high-pressure mercury lamp in an Oriel housing with quartz optics and dichroic mirrors (350–450 and 420–630 nm). Appropriate cutoff filters (Schott) were used. For the ESR experiments, LEDs with maximum outputs at 505 and 630 nm and a XeCl excimer laser ($\lambda = 308\text{ nm}$) were used.

Computations. Geometries were optimized using the B3LYP hybrid density functional^{40,41} as implemented⁴² in Gaussian 09⁴³ using the 6-311+G** basis set. Harmonic vibrational frequencies were computed at the B3LYP/6-311+G** level analytically. The B3LYP/6-311+G** geometries were employed for the computation of excitation energies and oscillator strengths using time-dependent DFT (TD-B3LYP/6-311+G**).⁴⁴

Vertical excitation energies were computed for PhNBN, PhB(N_2), and PhB(CO) at the B3LYP/6-311+G** geometry of the X^3A_2 state using internally contracted complete-active-space second-order perturbation theory (CASPT2) as described by Werner^{45,46} in conjunction with Dunning's correlation-consistent triple- ζ basis set (cc-pVTZ).⁴⁷ The active space chosen was identical to that used in earlier adiabatic MRMP2 computations, which were run, however, with the much smaller 6-31G* basis set.²⁵ In particular, the active space consisted of 12 orbitals (π_1 to π_6 of the phenyl ring as well as three p_π and three p_σ orbitals at the X–Y–Z terminus) and was occupied by 12 electrons. The correlated computations applied the frozen core approximation and were run using the Molpro program.^{48,49}

■ ASSOCIATED CONTENT

Supporting Information

The Supporting Information is available free of charge on the ACS Publications website at DOI: 10.1021/jacs.7b08497.

Additional UV/vis and ESR spectra, computed geometry of PhNBNC(O) (5), IR spectroscopic data, computed excitation energies, Cartesian coordinates, and complete refs 43 and 49 (PDF)

■ AUTHOR INFORMATION

Corresponding Author

*holger.bettinger@uni-tuebingen.de

ORCID

Holger F. Bettinger: 0000-0001-5223-662X

Notes

The authors declare no competing financial interest.

■ ACKNOWLEDGMENTS

This work was supported by the German Research Foundation (DFG). We thank Andreas Schnepf and Lars Wesemann for support and fruitful discussions. The computations were

performed on the BwForCluster JUSTUS. The authors acknowledge support by the state of Baden-Württemberg through bwHPC and the DFG through Grant INST 40/467-1 FUGG.

■ REFERENCES

- (1) van der Kerk, S. M.; Boersma, J.; van der Kerk, G. J. M. *Tetrahedron Lett.* **1976**, *17*, 4765–4766.
- (2) Schlögl, R.; Wrackmeyer, B. *Polyhedron* **1985**, *4*, 885–892.
- (3) Eisch, J. J.; Becker, H. P. *J. Organomet. Chem.* **1979**, *171*, 141–153.
- (4) Ramsey, B. G.; Anjo, D. M. *J. Am. Chem. Soc.* **1977**, *99*, 3182–3183.
- (5) Calhoun, G. C.; Schuster, G. B. *J. Org. Chem.* **1984**, *49*, 1925–1928.
- (6) Timms, P. L. *J. Am. Chem. Soc.* **1967**, *89*, 1629–1632.
- (7) Timms, P. L. *J. Am. Chem. Soc.* **1968**, *90*, 4585–4589.
- (8) Timms, P. L. *Acc. Chem. Res.* **1973**, *6*, 118–123.
- (9) Krasowska, M.; Bettinger, H. F. *Chem. - Eur. J.* **2016**, *22*, 10661–10670.
- (10) Pachaly, B.; West, R. *Angew. Chem., Int. Ed. Engl.* **1984**, *23*, 454–455.
- (11) Grigsby, W. J.; Power, P. P. *J. Am. Chem. Soc.* **1996**, *118*, 7981–7988.
- (12) Ito, M.; Tokitoh, N.; Kawashima, T.; Okazaki, R. *Tetrahedron Lett.* **1999**, *40*, 5557–5560.
- (13) Bissinger, P.; Braunschweig, H.; Damme, A.; Dewhurst, R. D.; Kupfer, T.; Radacki, K.; Wagner, K. *J. Am. Chem. Soc.* **2011**, *133*, 19044–19047.
- (14) Bissinger, P.; Braunschweig, H.; Kraft, K.; Kupfer, T. *Angew. Chem., Int. Ed.* **2011**, *50*, 4704–4707.
- (15) Curran, D. P.; Boussonnier, A.; Geib, S. J.; Lacote, E. *Angew. Chem., Int. Ed.* **2012**, *51*, 1602–1605.
- (16) Braunschweig, H.; Kruppenacher, I.; Légaré, M.-A.; Matler, A.; Radacki, K.; Ye, Q. *J. Am. Chem. Soc.* **2017**, *139*, 1802–1805.
- (17) Soleilhavou, M.; Bertrand, G. *Angew. Chem., Int. Ed.* **2017**, *56*, 10282–10292.
- (18) Kinjo, R.; Donnadieu, B.; Celik, M. A.; Frenking, G.; Bertrand, G. *Science* **2011**, *333*, 610–613.
- (19) Braunschweig, H.; Dewhurst, R. D.; Hupp, F.; Nutz, M.; Radacki, K.; Tate, C. W.; Vargas, A.; Ye, Q. *Nature* **2015**, *522*, 327–330.
- (20) Dahcheh, F.; Martin, D.; Stephan, D. W.; Bertrand, G. *Angew. Chem., Int. Ed.* **2014**, *53*, 13159–13163.
- (21) Ledet, A. D.; Hudnall, T. W. *Dalton Trans.* **2016**, *45*, 9820–9826.
- (22) Braunschweig, H.; Dewhurst, R. D.; Pentecost, L.; Radacki, K.; Vargas, A.; Ye, Q. *Angew. Chem., Int. Ed.* **2016**, *55*, 436–440.
- (23) Andrews, L.; Hassanzadeh, P.; Martin, J. M. L.; Taylor, P. R. *J. Phys. Chem.* **1993**, *97*, 5839–5847.
- (24) Bettinger, H. F. *J. Am. Chem. Soc.* **2006**, *128*, 2534–2535.
- (25) Bettinger, H. F. *J. Organomet. Chem.* **2006**, *691*, 4480–4485.
- (26) Krasowska, M.; Bettinger, H. F. *J. Am. Chem. Soc.* **2012**, *134*, 17094–17103.
- (27) Krasowska, M.; Bettinger, H. F. *Chem. - Eur. J.* **2014**, *20*, 12858–12863.
- (28) Bettinger, H. F.; Bornemann, H. *J. Am. Chem. Soc.* **2006**, *128*, 11128–11134.
- (29) Krasowska, M.; Edelman, M.; Bettinger, H. F. *J. Phys. Chem. A* **2016**, *120*, 6332–6341.
- (30) Finnerty, J.; Mitschke, U.; Wentrup, C. *J. Org. Chem.* **2002**, *67*, 1084–1092.
- (31) Hausser-Wallis, R.; Oberhammer, H.; Einholz, W.; Paetzold, P. O. *Inorg. Chem.* **1990**, *29*, 3286–3289.
- (32) Bettinger, H. F. *Organometallics* **2007**, *26*, 6263–6267.
- (33) Filthaus, M.; Schwertmann, L.; Neuhaus, P.; Seidel, R. W.; Oppel, I. M.; Bettinger, H. F. *Organometallics* **2012**, *31*, 3894–3903.

- (34) Bettinger, H. F.; Filthaus, M.; Bornemann, H.; Oppel, I. M. *Angew. Chem., Int. Ed.* **2008**, *47*, 4744–4747.
- (35) Wasserman, E.; Smolinsky, G.; Yager, W. A. *J. Am. Chem. Soc.* **1964**, *86*, 3166–3167.
- (36) Trozzolo, A. M.; Murray, R. W.; Wasserman, E. *J. Am. Chem. Soc.* **1962**, *84*, 4990–4991.
- (37) Mennekes, T.; Paetzold, P. *Z. Anorg. Allg. Chem.* **1995**, *621*, 1175–1177.
- (38) Dunkin, I. R. *Matrix-Isolation Techniques*; Oxford University Press: Oxford, U.K., 1998.
- (39) Griffin, M.; Muys, A.; Noble, C.; Wang, D.; Eldershaw, C.; Gates, K. E.; Burrage, K.; Hanson, G. R. *Mol. Phys. Rep.* **1999**, *26*, 60–84.
- (40) Becke, A. D. *J. Chem. Phys.* **1993**, *98*, 5648–5652.
- (41) Lee, C.; Yang, W.; Parr, R. G. *Phys. Rev. B: Condens. Matter Mater. Phys.* **1988**, *37*, 785–789.
- (42) Stephens, P. J.; Devlin, F. J.; Chabalowski, C. F.; Frisch, M. J. *J. Phys. Chem.* **1994**, *98*, 11623–11627.
- (43) Frisch, M. J.; et al. *Gaussian 09*, revision D.01; Gaussian, Inc.: Wallingford, CT, 2009.
- (44) Stratmann, R. E.; Scuseria, G. E.; Frisch, M. J. *J. Chem. Phys.* **1998**, *109*, 8218–8224.
- (45) Werner, H.-J. *Mol. Phys.* **1996**, *89*, 645–661.
- (46) Celani, P.; Werner, H.-J. *J. Chem. Phys.* **2000**, *112*, 5546–5557.
- (47) Dunning, T. H. *J. Chem. Phys.* **1989**, *90*, 1007–1023.
- (48) Werner, H.-J.; Knowles, P. J.; Knizia, G.; Manby, F. R.; Schütz, M. *WIREs Comput. Mol. Sci.* **2012**, *2*, 242–253.
- (49) Werner, H.-J.; et al. *MOLPRO, a Package of ab Initio Programs*, version 2015.1; see <http://www.molpro.net>.